Formation of cold molecular ions by radiative processes in cold ion-atom collisions

Arpita Rakshit[1] and Bimalendu Deb[1,2]

[1]*Department of Materials Science, Indian Association for the Cultivation of Science, Jadavpur, Kolkata 700032, India*

[2]*Raman Center for Atomic, Molecular and Optical Sciences, Indian Association for the Cultivation of Science, Jadavpur, Kolkata 700032, India*

(Received 25 September 2010; published 7 February 2011)

We discuss theoretically ion-atom collisions at low energy and predict the possibility of the formation of a cold molecular ion by photoassociation. We present results from radiative homo- and heteronuclear atom-ion cold collisions that reveal threshold behavior of atom-ion systems.

DOI: 10.1103/PhysRevA.83.022703 PACS number(s): 34.10.+x, 34.70.+e, 34.50.Cx, 42.50.Ct

I. INTRODUCTION

Molecular ions are important for a variety of fundamental studies in physics. For instance, it is proposed that cold molecular ions would be useful for measuring electron dipole moment (EDM) [1,2]. The study of cold molecular ions has relevance in diverse areas such as metrology [3,4] and astrochemistry [5]. Recently, molecular ions are cooled into rovibrational ground states by all optical [6], laser, and sympathetic cooling methods [7,8]. A large variety of diatomic and triatomic molecular ions are also cooled by sympathetic methods [9–11]. Other methods such as photoassociative ionization [12–16], buffer gas [17], and rotational cooling [18] have been widely used for producing low-energy molecular ions. Since cooling of neutral atoms and atomic ions down to sub-millikelvin temperature regime is possible with currently available technology of laser cooling, it is now natural to ask ourselves: Is it possible to form cold molecular ions by atom-ion cold collisions? Recent progress in developing hybrid traps [19–22] where both atomic ions and neutral atoms can be simultaneously confined provides new opportunity for exploring ion-atom quantum dynamics and charge-transfer reactions at ultralow temperatures. As neutral cold atoms can be photoassociated [23] into cold dimers, the same association method should also apply to atoms colliding with atomic ions forming cold molecular ions. Understanding ion-atom cold collision [20–22,24–32] is important for realizing a charged quantum gas, studying charge transport [33] at low temperature, exploring polaron physics [34–36], and producing ion-atom bound states [37] and cold molecular ions [6–8].

Although in recent times there have been several studies on ion-atom cold collisions, formation of molecular ions by photoassociation (PA) has yet to be demonstrated. There are qualitative differences between atom-atom and ion-atom PA. In contrast to atom-atom PA, heteronuclear atom-ion PA is accompanied by charge transfer. Neutral atom-atom PA involves excited diatomic molecular states which in the separated-atom limit correspond of one ground (S) atom and the other excited (P) atom. Heteronuclear atom-ion PA may involve excited molecular states which asymptotically correspond to separated atoms and ions both belonging to S electronic states. The long-range potentials of an ion-atom system behave quite differently from those of a neutral atom-atom system.

Here we show that it is possible to form translationally and rotationally cold molecular ions by PA. We specifically focus on heteronuclear radiative processes. However, we study in general both homo- and heteronuclear ion-atom cold collisions to reveal the contrast between the two processes. At ultralow collision energies, radiative charge transfer processes dominate over nonradiative ones. Starting from a cold alkaline-earth-metal ion and an ultracold alkali-metal atom (such as an atom of alkali-metal Bose-Einstein condensates) as the initial reactants, formation of a ground-state molecular ion requires a three-step radiative reaction process. In the first step, the ion-atom pair in the continuum of the excited electronic state undergoes radiative charge transfer to the continuum of the ground electronic state. In the second step, the ground continuum ion-atom pair is exposed to laser radiation of appropriate frequency to photoassociate them into an excited molecular ion. In the third and final step, another laser is used to stimulate the excited molecular ion to deexcite into a particular rovibrational level of ground electronic state. Since a molecular ion is formed from an initially cold atom and an ion, the molecular ion remains translationally and rotationally cold. One noteworthy feature of this method is the selectivity of a low-lying rotational level. We present selective results on elastic and radiative charge-transfer scattering cross sections for both homo- and heteronuclear ion-atom collisions. For model potentials of a $(LiBe)^+$ system, we calculate the PA rate of formation of a $LiBe^+$ molecular ion.

This paper is organized in the following way. In Sec. II, we describe our model focusing on possible elastic and inelastic processes. Results are presented and discussed in Sec. III. In the last section we draw our conclusions.

II. ELASTIC AND INELASTIC PROCESSES

We consider cold collision of an alkali-metal atom A with an alkaline-earth-metal ion B^+ in a hybrid trap. The possible elastic and inelastic processes are schematically depicted in Fig. 1. These are (1) elastic collision between A and B^+, (2) an e^- from A may hop to B^+ provided they are close enough to each other, forming a ground-state pair of ion A^+ and atom B, (3) an atom-ion pair in the excited continuum may decay spontaneously to a bound level of lower electronic state, (4) an excited atom-ion pair may be transferred to a ground electronic bound state by a stimulated emission process, (5) the ground-state atom-ion pair may undergo elastic collision, (6) the ground pair may be photoassociated in the presence of appropriate laser radiation to form an excited molecular

 ©2011 American Physical Society

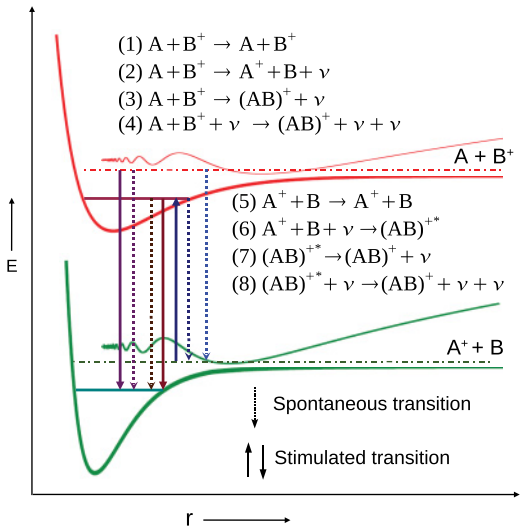

FIG. 1. (Color online) Schematic diagram of possible physical processes which can take place during atom-ion collisions at low energy.

ion, (7) this excited molecular ion may decay sponataneously either to a ground bound state or to a continuum, (8) an excited bound state may be transferred to a ground bound state by a stimulated emission process.

To illustrate atom-ion radiative cold collisions, we consider a model system of $^7\mathrm{Li} + \mathrm{Be}^+$ undergoing elastic and radiative charge-transfer collisions. The possible experimental situation can be imagined as a single Be^+ ion immersed in a Bose-Einstein condensate of ^{7}Li atoms in a hybrid trap. The molecular potentials $1^1\Sigma^+$ (ground) and $2^1\Sigma^+$ (excited) of the $(\mathrm{LiBe})^+$ system as shown in Fig. 2 (top inset) asymptotically go to $^1S + {}^1S$ ($\mathrm{Li}^+ + \mathrm{Be}$) and $^2S + {}^2S$ ($\mathrm{Be}^+ + \mathrm{Li}$), respectively. We construct model potentials $1^1\Sigma^+$ (ground) and $2^1\Sigma^+$ (excited) of the $(\mathrm{LiBe})^+$ system using spectroscopic constants given in Ref. [38]. The short-range potential is approximated using Morse potential and the long-range potential [30,31] is

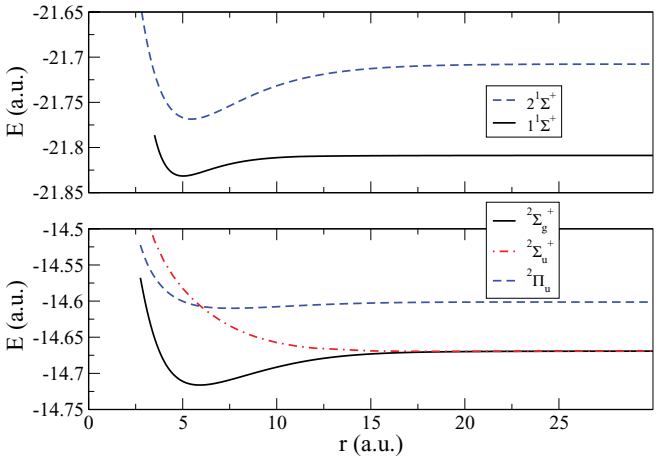

FIG. 2. (Color online) (Top) $1^1\Sigma^+$ (solid line) and $2^1\Sigma^+$ (dashed line) model potentials of a $(\mathrm{LiBe})^+$ system. (Bottom) $^2\Sigma_g^+$ (solid line), $^2\Sigma_u^+$ (dash-dotted line), and $^2\Pi_u$ (dashed line) potentials of Li_2^+.

TABLE I. Dissociation energies D_e in a.u., equilibrium positions r_e, and the effective lengths β_4 in bohr radius for excited- and ground-state potentials $[V(r)]$ of $(\mathrm{LiBe})^+$ and $(\mathrm{LiLi})^+$ systems.

System	$V(r)$	D_e	r_e	β_4
$(\mathrm{LiBe})^+$	$2^1\Sigma^+$	0.06	5.46	1083.4
$(\mathrm{LiLi})^+$	$^2\Pi_u$	0.01	7.50	1019.8
$(\mathrm{LiBe})^+$	$1^1\Sigma^+$	0.02	5.03	515.9
$(\mathrm{LiLi})^+$	$^2\Sigma_g^+$	0.05	6.00	1019.8

given by the expression

$$V(r) = -\frac{1}{2}\left(\frac{C_4}{r^4} + \frac{C_6}{r^6} + \cdots\right), \tag{1}$$

where C_4, C_6 correspond to dipole, quadrupole polarizabilities of the atom concerned. The polarization interaction falls off much more slowly than van der Waals interaction which represents the long-range part of interaction between neutral atoms. Hence, collision between atom and ion is dominated by the long-range polarization interaction. The qualitative feature of this long-range interaction of atom-ion is governed by the effective length which is given by $\beta_4 = \sqrt{2\mu C_4/\hbar^2}$ where μ is the reduced mass. The short-range and long-range parts of the potentials are smoothly joined by a spline.

Since Li^+ may be formed due to a charge-transfer collision between Be^+ and Li, we need to consider the interaction between this Li^+ and other Li atoms present in the condensate. The data for $^2\Sigma_g^+$, $^2\Sigma_u^+$, and $^2\Pi_u$ potentials of Li_2^+ are taken from Ref. [39]. Dissociation energy D_e, equilibrium position r_e, and effective range β_4 of the ground and excited state potentials of the $(\mathrm{LiBe})^+$ and LiLi^+ systems are given in Table I. A comparison of potentials of these two systems reveals that the ground-state potential $1^1\Sigma^+$ of $(\mathrm{LiBe})^+$ is much shallower than the $^2\Sigma_g^+$ potential of Li_2^+. The equilibrium positions of both ground- and excited-state potentials of the $(\mathrm{LiBe})^+$ system lie almost at the same separation. Unlike the asymptotic behavior of the excited $2^1\Sigma^+$ potential of the $(\mathrm{LiBe})^+$ system, the excited-state potential $^2\Pi_u$ of homonuclear Li_2^+ molecular ion asymptotically corresponds to one Li^+ ion in the electronic ground S state and one neutral Li atom in the excited P state. The equilibrium positions r_e of ground- and excited-state potentials of Li_2^+ system are shifted by 1.5 bohr radius. For the $(\mathrm{LiBe})^+$ system, we notice that β_4 of the excited $(2^1\Sigma^+)$ potential is almost twice that of the ground $(1^1\Sigma^+)$ potential.

Let us first consider cold collision between Li and Be^+ with both of them being in ^2S electronic state. So, our initial system corresponds to the continuum of $2^1\Sigma^+$ potential. Due to charge-transfer collision a neutral Be atom and a Li^+ ion are generated. In the separated two-particle limit of this system, dipole transition to ground state at the single-particle level is forbidden. Furthermore, since at low energy nonradiative charge transfer is suppressed, the dominant inelastic channel is the radiative charge transfer transition that occurs at intermediate or short separations. Electronic transition dipole moment between two ionic molecular electronic states vanishes at large separation. Therefore, transitions occur at short range where hyperfine interaction is negligible in comparison to

central (Coulombic) interaction. The total molecular angular momentum is given by $\vec{J} = \vec{S} + \vec{L} + \vec{\ell}$, where S and L are the total electronic spin and orbital quantum number, respectively, and ℓ stands for the angular quantum number of the relative motion of the two atoms. For the particular model for the $(LiBe)^+$ system chosen here, we have $L = 0$ and $S = 0$ for both the ground and the excited electronic states. Thus, here the total angular momenta for both the ground and the excited states are given by $J = \ell$. However, it is more appropriate to denote total angular quantum number of a molecular bound state by J and that of the continuum or collisional state of this atom-ion system by simply ℓ. The parity selection rule for the electric dipole transition between the ground and the excited state dictates $\Delta J = \pm 1$.

To investigate ion-atom elastic scattering and free-bound transitions, we need to calculate continuum wave functions which are obtained by solving the partial-wave Schrödinger equation given by

$$\left[\frac{d^2}{dr^2} + k^2 - \frac{2\mu}{\hbar^2}V(r) - \frac{\ell(\ell+1)}{r^2}\right]\psi_\ell(kr) = 0, \qquad (2)$$

where r is the ion-atom separation. The wave function $\psi_\ell(kr)$ has the asymptotic form $\psi_\ell(kr) \sim \sin[kr - \ell\pi/2 + \eta_l]$, with $\eta_\ell(k)$ being the phase shift for ℓth partial wave. The total elastic scattering cross section is expressed as

$$\sigma_{el} = \frac{4\pi}{k^2}\sum_{\ell=0}^{\infty}(2\ell+1)\sin^2(\eta_\ell), \qquad (3)$$

where $k = \sqrt{(2mE/\hbar^2)}$. As the energy gradually increases more and more partial waves start to contribute to total elastic scattering cross sections and the scattering cross section at large energy is [30]

$$\sigma_{\rm el} \sim \pi\left(\frac{\mu C_4^2}{\hbar^2}\right)^{\frac{1}{3}}\left(1 + \frac{\pi^2}{16}\right)E^{-\frac{1}{3}}. \qquad (4)$$

As $k \to 0$, according to Wigner threshold laws $\eta_\ell(k) \sim k^{2\ell+1}$ if $\ell \leqslant (n-3)/2$ with n being the exponent of long-range potential behaving as $\sim 1/r^n$ as $r \to \infty$. If $\ell > (n-3)/2$, then the threshold law is $\eta_\ell(k) \sim k^{n-2}$. Since the long-range part of ground as well as excited ion-atom potentials goes as $\sim 1/r^4$ as $r \to \infty$, Wigner threshold laws tell us that s-wave ($\ell = 0$) ion-atom scattering cross section should be independent of k while all the higher partial-wave scattering cross sections should go as $\sim k^2$ in the limit $k \to 0$.

Ion-atom inelastic collisions are mainly of two kinds—charge-transfer reactions and radiative- or photoassociative transfer [40–44]. The radiative charge-transfer cross section [40–42] is given by

$$\sigma_{\rm ct} = \int_{\omega_{\rm min}}^{\omega_{\rm max}} \frac{d\sigma_{\rm ct}}{d\omega}d\omega, \qquad (5)$$

where ω is the angular frequency of emitted photon and

$$\frac{d\sigma_{\rm ct}}{d\omega} = \frac{8\omega^3\pi^2}{3c^3k_m^2}\sum_l\left[\ell M^2_{\ell,\ell-1}(k_m,k_n) + (\ell+1)M^2_{\ell,\ell+1}(k_m,k_n)\right], \qquad (6)$$

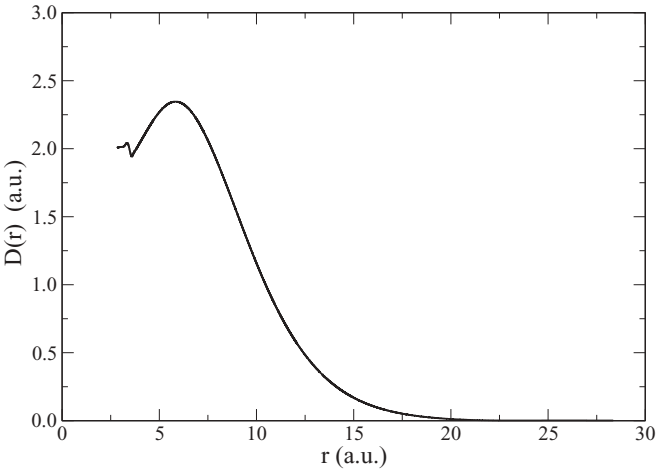

FIG. 3. Radial transition dipole matrix element as a function of separation r for a $(LiBe)^+$ system.

where

$$M_{\ell,\ell'}(k_m,k_n) = \int_0^\infty dr\,\psi_\ell^m(k_m r)D(r)\psi_{\ell'}^n(k_n r). \qquad (7)$$

Here $D(r)$ is the magnitude of the molecular transition dipole moment. Here $k_m = \sqrt{2\mu\,[E - V_m(\infty)]}$ and $k_n = \sqrt{2\mu\,[E - V_n(\infty) - \hbar\omega]}$ are the momentum of the entrance and exit channels, respectively; and E is collision energy of the entrance (m) channel. V_m and V_n are the potential energies of the entrance (m) and exit (n) channels, respectively. $\psi_\ell^i(k_i r)$ is the wave function of ℓth partial wave for ith channel of momenum k_i. The total radiative transfer [41] from the upper state (m) to the lower state (n) is given by

$$\sigma_{rt} = \frac{\pi}{k_m^2}\sum_\ell^\infty(2\ell+1)[1 - \exp(-4\zeta_\ell)], \qquad (8)$$

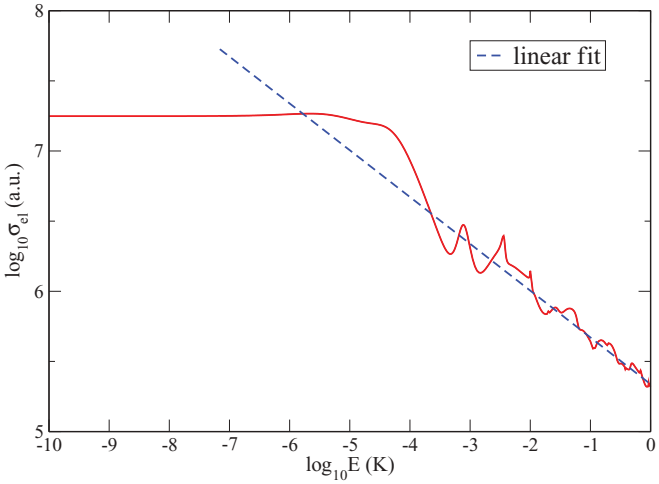

FIG. 4. (Color online) Total elastic scattering cross-section $\sigma_{\rm el}$ for a Li + Be^+ ($2^1\Sigma^+$) collision is plotted against collision energy E in K. The dashed curve is a linear fit for energies greater than 10^{-6} K.

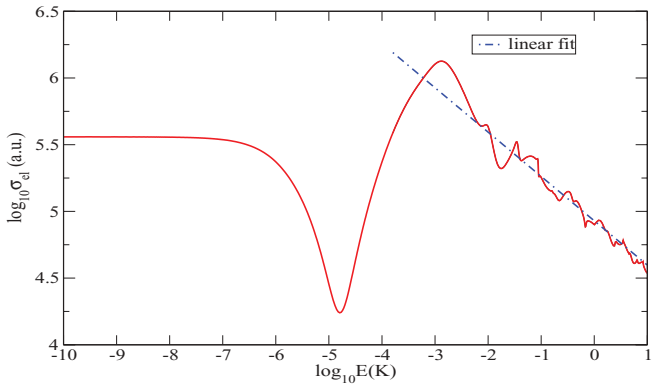

FIG. 5. (Color online) Same as in Fig. 4 but for $Li^+ + Be$ ($1^1\Sigma^+$).

where

$$\zeta_\ell = \frac{\pi}{2}\int_0^\infty |\psi_\ell^m(k_m r)|^2 A_{nm}(r)\,dr \tag{9}$$

is a phase shift and

$$A_{nm}(r) = \frac{4}{3}D^2(r)\frac{|V_n(r) - V_m(r)|^3}{c^3} \tag{10}$$

is the transition probability.

The ground continuum atom-ion pair, formed by radiative charge-transfer process, can be photoassociated to form an excited molecular ion. This process is basically one photon PA process. The PA rate coefficient is given by

$$K_{\rm PA} = \left\langle \frac{\pi v_r}{k^2}\sum_{\ell=0}^{\infty}(2\ell+1)|S_{\rm PA}(E,\ell,w_L)|^2 \right\rangle, \tag{11}$$

where $v_r = \hbar k/\mu$ is the relative velocity of the two particles and $\langle\cdots\rangle$ implies averaging over thermal velocity distribution. Here $S_{\rm PA}$ is an S matrix element given by

$$|S_{\rm PA}|^2 = \frac{\gamma\Gamma_\ell}{\delta_E^2 + (\Gamma_\ell+\gamma)^2/4}, \tag{12}$$

where $\delta_E = E/\hbar + \delta_{vJ}$, $\delta_{vJ} = \omega_L - \omega_{vJ}$, with $E_{vJ} = \hbar\omega_{vJ}$ being binding energy of the excited rovibrational state, ω_L being the laser frequency, and γ being the spontaneous line

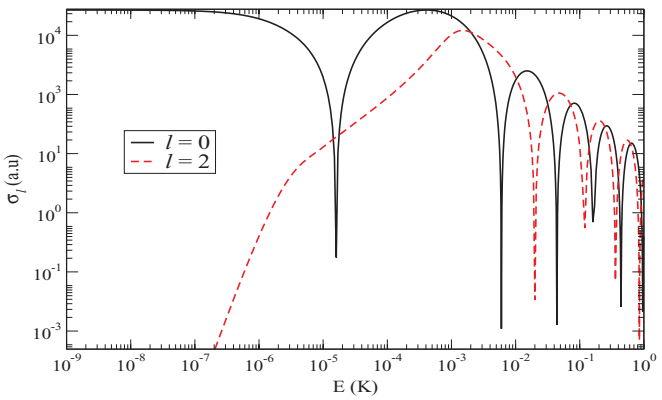

FIG. 6. (Color online) Partial-wave cross sections for $Li^+ + Be$ ($1^1\Sigma^+$) collision are plotted as a function of E (in K) for $\ell = 0$ (solid line) and $\ell = 2$ (dashed line).

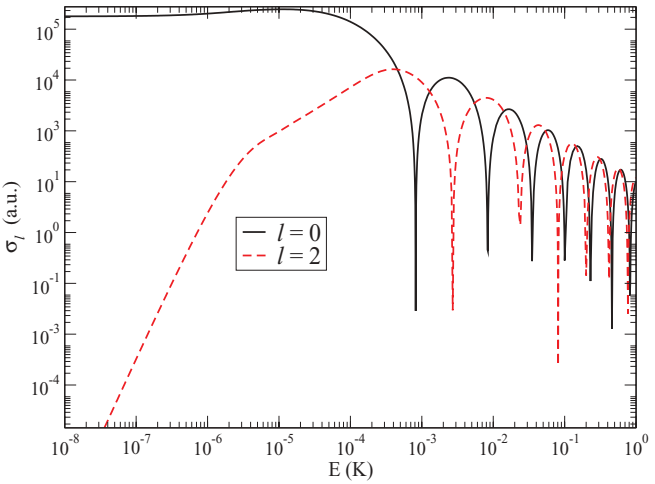

FIG. 7. (Color online) Same as in Fig. 6 but for $Li + Li^+$ ground-state collision in $^2\Sigma_g$ state.

width. Thus, the PA rate is primarily determined by partial-wave stimulated line width Γ_ℓ given by

$$\hbar\Gamma_\ell = \frac{8\pi^2 I}{3\epsilon_0 c}h(J,\ell)|D_{vJ,l}|^2, \tag{13}$$

where

$$D_{vJ,l} = \langle\phi_{vJ}|D(r)|\psi_\ell(kr)\rangle \tag{14}$$

is the radial transition dipole matrix element between the continuum and bound state wave functions $\psi_\ell(kr)$ and $\phi_{vJ}(r)$, respectively. I is the intensity of the laser, c is the speed of light, and ϵ_0 is the vacuum permittivity. Here $h(J,\ell)$ is the Hönl London factor [45], which in the present context is given by

$$h(J,\ell) = (1 + \delta_{\Lambda'0} + \delta_{\Lambda''0} - 2\delta_{\Lambda'0}\delta_{\Lambda''0}) \times (2J+1)(2\ell+1)\begin{pmatrix} J & 1 & \ell \\ -\Lambda' & \Lambda'-\Lambda'' & \Lambda'' \end{pmatrix}^2, \tag{15}$$

where Λ' and Λ'' are the projections of the total electronic orbital angular momentum of the excited and ground states,

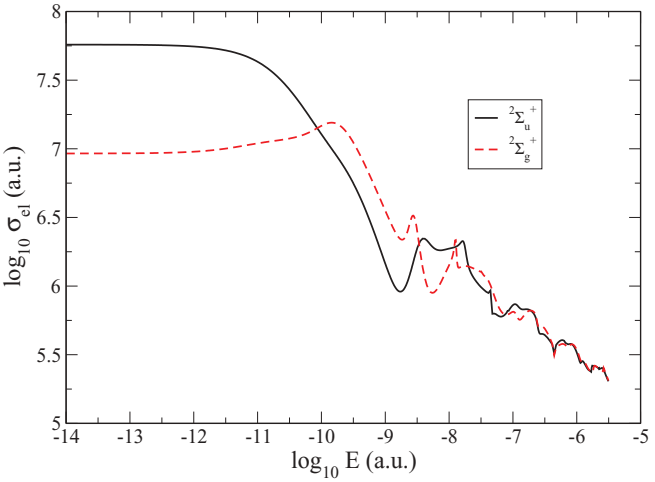

FIG. 8. (Color online) Same as in Fig. 4 but for $Li + Li^+$ collision in $^2\Sigma_g^+$ (dashed line) and $^2\Sigma_u^+$ (solid line) potentials.

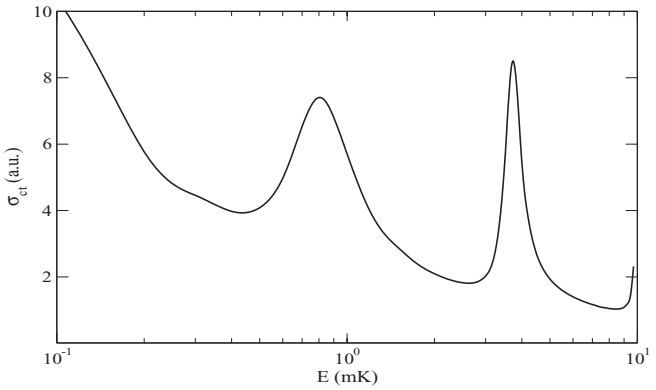

FIG. 9. Charge-transfer scattering cross section σ_{ct} (in a.u.) of the $(LiBe)^+$ system is plotted against collisional energy E (in mK).

respectively, on molecular axis and $(\cdots)$ is the Wigner $3j$ symbol. The spontaneous line width γ of the excited state (v, J) is given by

$$\hbar\gamma = \frac{1}{3\pi\epsilon_0 c^3}\left[\int (\Delta E)^3 |\langle\phi_{vJ} \mid D(r) \mid \psi_E\rangle|^2 dE + \sum_{v',J'} \Delta^3_{v'J'} |\langle\phi_{vJ} \mid D(r) \mid \phi_{v'J'}\rangle|^2\right], \quad (16)$$

where $\Delta E = (E_{vJ} - E)/\hbar$, $\Delta_{v'J'} = (E_{vJ} - E_{v',J'})/\hbar$, ψ_E is the scattering wave function, and $\mid \phi_{v'J'}\rangle$ stands for all the final bound states to which the excited state can decay spontaneously.

III. RESULTS AND DISCUSSION

Standard renormalized Numerov-Cooley method [46] is used to calculate the bound- and scattering-state wave functions. The molecular transition dipole matrix element of the $(LiBe)^+$ system is calculated using GAMESS. This matrix element strongly depends upon separation and goes to zero at a large r as shown in Fig. 3. In Figs. 4 and 5, we have plotted the excited- and ground-state elastic scattering cross section σ_{el} as a function of energy E for $Li + Be^+$ and $Li^+ + Be$ collisions, respectively. We find that at least 35 partial waves are required to get converging results on elastic scattering for

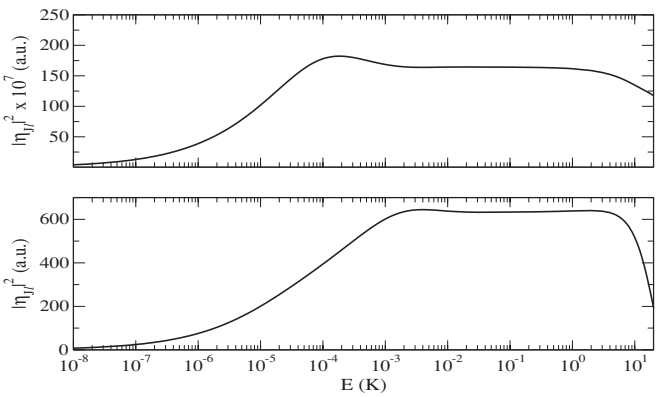

FIG. 10. Square of Franck Condon overlap integral $|\eta_{J\ell}|^2$ (in a.u.) for Li-Li^+ (top) and $(LiBe)^+$ (bottom) is plotted against E (in K). In the top panel, $|\eta_{J\ell}|^2$ is mutiplied by a factor of 10^7.

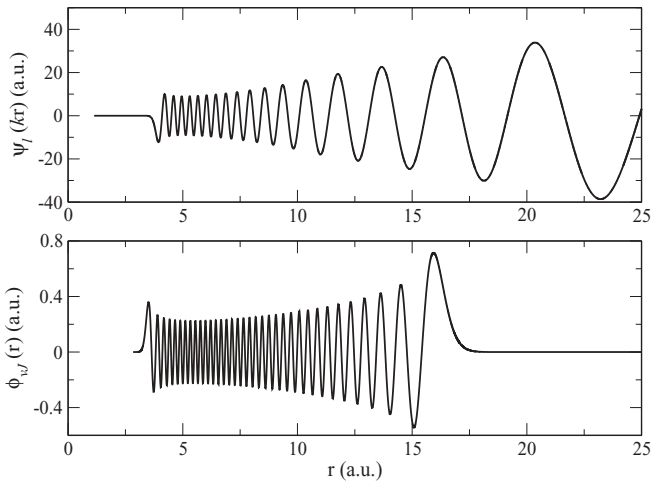

FIG. 11. Energy-normalized s-wave ground scattering (top) and unit normalized excited bound (bottom) wave functions of the $(LiBe)^+$ system are plotted as a function of separation r.

energies higher than 1 μK. In our calculations we have used 51 partial waves. At high energies, for both the cases, σ_{el} decreases as $E^{-\frac{1}{3}}$. The proportionality constant c in the expression $\sigma_{el}(E \to \infty) = cE^{-\frac{1}{3}}$ calculated using Eq. (4) for excited $2^1\Sigma^+$ and ground $1^1\Sigma^+$ potentials is 2936 and 1091 a.u., respectively, whereas linear fit to σ_{el} vs E curves provides $c = 3548$ and 1335 a.u., respectively. Figures 6 and 7 exhibit s- and d-wave partial scattering cross section as a function of energy for $Li^+ + Be$ and $Li + Li^+$ collisions, respectively. These figures show that the Wigner threshold behavior begins to set in as the collision energy decreases below 0.1 μK. In Fig. 8, we have plotted total elastic scattering cross section for $Li + Li^+$ collisions in $^2\Sigma_g^+$ and $^2\Sigma_u^+$ potentials.

Starting from the low-energy continuum state of $Li + Be^+$ collision in the $2^1\Sigma^+$ potential, there arise two possible radiative transitions by which the system can go to the ground electronic state $1^1\Sigma^+$. One is continuum-continuum and the other is continuum-bound dipole transition. The transition dipole moment as a function of separation as shown in Fig. 3 shows that the dipole transition probability will vanish as the

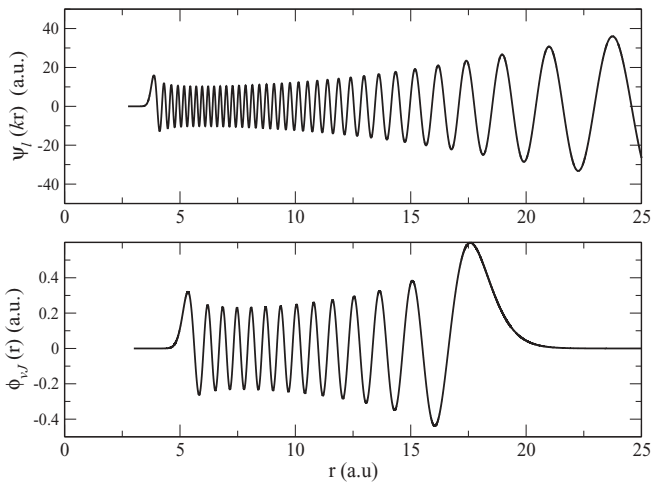

FIG. 12. Same as in Fig. 11 but for the Li-Li^+ system.

separation increases above $20a_0$. So a dipole trasition has to take place at short separations. Let us consider radiative transfer processes from the upper ($2^1\Sigma^+$) to the lower ($1^1\Sigma^+$) state of $(LiBe)^+$. We then need to apply the formulas (5) and (8) where $m \equiv 2^1\Sigma^+$ and $n \equiv 1^1\Sigma^+$ in our case. Continuum-continuum charge transfer cross section σ_{ct} between $2^1\Sigma^+$ and $1^1\Sigma^+$ states of $(LiBe)^+$ system is plotted against E in Fig. 9. We evaluate the photoassociative (continuum-bound) transfer cross section by subtracting σ_{ct} from the total radiative transfer cross section σ_{rt} calculated using the formula (8). At energy $E = 0.1$ mK, σ_{ct} and the photoassociative transfer cross section are found to be 10.39 and 0.03 a.u., respectively. Thus, we infer that the continuum-continuum radiative charge-transfer process dominates over the radiative association process. Also, we notice that σ_{ct} is smaller than both the excited- and the ground-state elastic scattering cross sections σ_{el} (as given in Figs. 4 and 5, respectively) by several orders of magnitude.

Molecular dipole transitions between two rovibrational states or between continuum and bound states are governed by Franck-Condon principle. According to this principle, for excited vibrational (bound) states, bound-bound or continuum-bound transitions primarily occur near the turning points of bound states. In general, highly excited vibrational-state wave functions of diatomic molecules or molecular ions have their maximum amplitude near the outer turning points. Spectral intensity is proportional to the overlap integral. This means that the spectral intensity for a continuum-bound transition would be significant when the continuum state has a prominent node near the outer turning point of the bound state. For transitions between two highly excited bound states, the Franck-Condon principle implies that the probability of such transitions would be significant when the outer turning points of these two bound states lie nearly at the same separation. The top panel of Fig. 10 shows the variation of the square of the Franck Condon overlap integral $|\eta_{J\ell}|^2$ between the ground s-wave ($\ell = 0$) scattering and the excited rovibrational ($v = 26, J = 1/2$) states of the Li-Li^+ system as a function the collision energy E. The bottom panel of Fig. 10 displays the same as in the top panel but for the $(LiBe)^+$ system with $v = 68$ and $J = 1$. The excited rovibrational state $v = 26, J = 1/2$ of Li-Li^+ is very close to dissociation threshold, while the excited rovibrational state $v = 68, J = 1$ of the $(LiBe)^+$ system is a deeper bound state. These two excited states are so chosen such that the free-bound Franck-Condon overlap integrals for both the systems become significant. Comparing these two plots, we find that $|\eta_{J\ell}|^2$ of the Li-Li^+ system is smaller than that of the $(LiBe)^+$ system by seven orders of magnitude. To understand why the values $|\eta_{J\ell}|^2$ for the two systems are so different, we plot the the energy-normalized s-wave ground scattering and the bound-state wave functions of the $(LiBe)^+$ system in Fig. 11 and those of the Li-Li^+ system in Fig. 12. A comparison of Figs. 11 and 12 reveals that, while in the case of $(LiBe)^+$ the maximum of the excited bound-state wave function near the outer turning point coincides nearly with a prominent antinode of the scattering wave function, in the case of Li-Li^+ the maximum of the bound-state wave function near the outer turning point almost coincides with a minimum (node) of the scattering wave function. These results

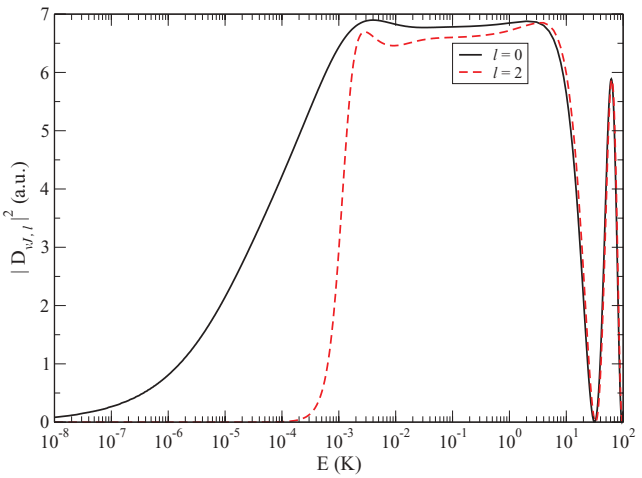

FIG. 13. (Color online) Square of free-bound radial transition dipole moment ($|D_{vJ,l}|^2$) (in a.u.) for ground continuum states with $\ell = 0$ (solid line) and $\ell = 2$ (dashed line) and excited bound rovibrational level with $v = 68$ and $J = 1$.

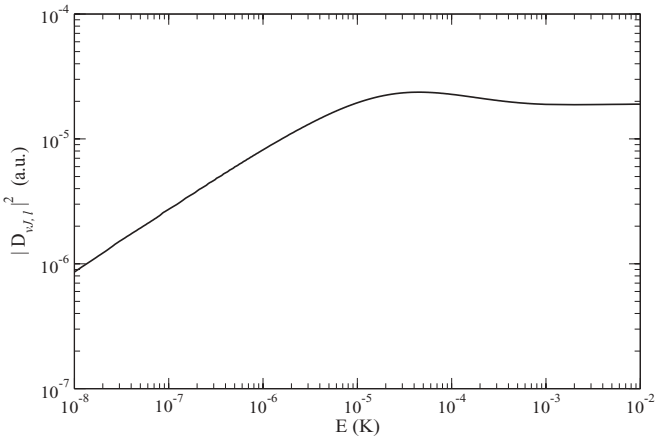

FIG. 14. Same as in Fig. 13 but for excited continuum state with $\ell = 0$ and ground rovibrational state with $v = 36$ and $J = 1$.

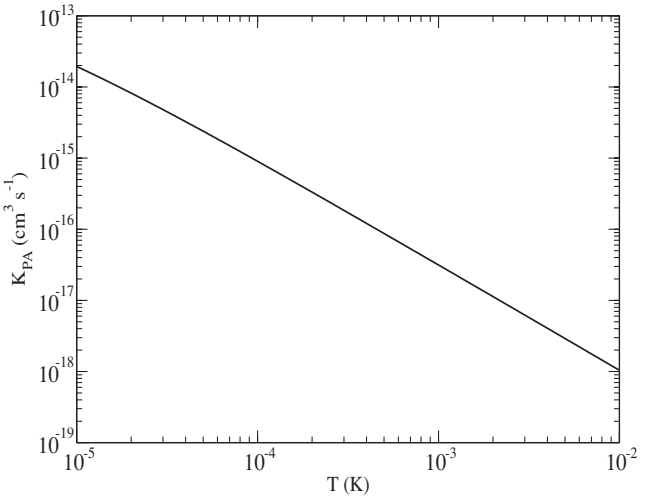

FIG. 15. Rate of PA K_{PA} (in cm^3 s^{-1}) of $(LiBe)^+$ is plotted against temperature (in K) at $I = 1$ W/cm^2 and $\delta_{vJ} = \omega_L - \omega_{vJ} = 0$.

indicate that the possibility of the formation of the excited $LiLi^+$ molecular ion via PA is much smaller than that of the $(LiBe)^+$ ion. We henceforth concentrate on PA of the $(LiBe)^+$ system only.

We next explore the possibility of PA in Li^+-Be cold collision in the presence of laser light. As discussed before, continuum-bound molecular dipole transition matrix element depends on the degree of overlap between continuum and bound states. PA rate (11) is proportional to the square of free-bound radial transition dipole moment element $|D_{vJ,l}|^2$. In Fig. 13 we plot $|D_{vJ,l}|^2$ against E for s- ($\ell = 0$) and d-wave ($\ell = 2$) ground-scattering states and $v = 68$, $J = 1$ excited molecular state. It is clear from this figure that the contributions of both $\ell = 0$ and $\ell = 2$ partial waves are comparable above energy corresponding to 0.1 mK. At lower energy ($E < 0.1$ mK), only the s wave makes finite contribution to the dipole transition. Figure 14 exhibits $|D_{vJ,l}|^2$ as a function of E for the transition from the s-wave ($\ell = 0$) scattering state of the excited $(2^1\Sigma^+)$ continuum to the ground $(1^1\Sigma^+)$ rovibrational state with $v = 36$, $J = 1$. A comparison between Figs. 13 and 14 reveals that the probability for the transition from the upper continuum to the ground bound state is smaller by several orders of magnitude than that from ground continuum to an excited bound state. In Fig. 15, we have plotted the rate of PA $K_{\rm PA}$ as a function of temperature T for laser frequency tuned at PA resonance. The ion-atom PA rate as depicted in Fig. 15 is comparable to the typical values of rate of neutral atom-atom PA at low laser intesities. In Fig. 16 we have plotted the rate of PA as a function of laser intensity at a fixed temperature $T = 0.1$ mK to show the saturation effect that occurs around intensity $I = 50$ kW/cm^2. Thus, the formation of the excited $(LiBe)^+$ molecular ion by photoassociating colliding Li^+ with Be with a laser of moderate intensity appears to be a feasible process.

Now we discuss the possibility of the formation of a ground-state molecular ion by a stimulated Raman-type process by applying a second laser tuned near a bound-bound transition between the excited and the ground potentials. Let us consider

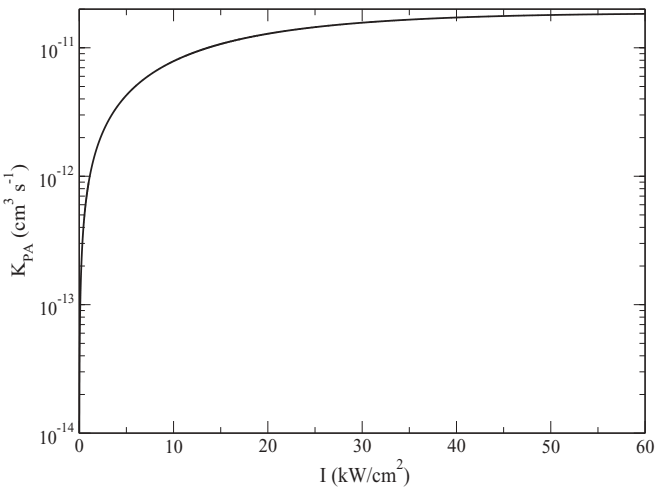

FIG. 16. $K_{\rm PA}$ (in cm^3 s^{-1}) of $(LiBe)^+$ is plotted as a function of laser intensity I (in kW/cm^2) at temperature $T = 0.1$ mK with laser tuned at PA resonance.

TABLE II. Rovibrational energy (E_{vJ}) and inner (r_i) and outer turning points (r_o) of two selected bound states of $(LiBe)^+$ molecular ion—one bound state in excited $(2^1\Sigma^+)$ and the other in ground $(1^1\Sigma^+)$ potential. The energy E_{vJ} is measured from the threshold of the respective potential.

Potential	v	J	E_{vJ} (a.u.)	r_i (a.u.)	r_o (a.u.)
$2^1\Sigma^+$	68	1	-3.30×10^{-3}	3.4	16.3
$1^1\Sigma^+$	29	0	-0.25×10^{-3}	3.8	16.6

two selected bound states whose salient features are given in Table II. The outer turning points of these two bound states almost coincide, implying the existence of a large Franck-Condon overlap between them. To see whether coherent laser coupling between these two bound states is possible or not, we calculate Rabi frequency Ω given by

$$\hbar\Omega = \left(\frac{I}{4\pi c\epsilon_0}\right)^{\frac{1}{2}} |\langle v, J \,|\, \vec{D}(r)\cdot\hat{\epsilon}_L \,|\, v', J'\rangle|, \qquad (17)$$

where $\hat{\epsilon}_L$ is the unit vector of laser polarization and $|\,v, J\rangle$ and $|\,v', J'\rangle$ are the two bound states with $\langle r\,|\,v, J\rangle = \phi_{vJ}(r)$. Rabi frequency corresponding to this bound-bound transition is found to be 285 MHz for laser intensity $I = 1$ kW/cm^{-2}. Comparing this value with the spontaneous line width $\gamma = 57$ kHz of the excited bound state calculated using the formula (16), we infer that even at a low laser intensity which is far below the saturation limit, bound-bound Rabi frequency Ω exceeds γ by several orders of magnitude. This indicates that it may be possible to form ground molecular ion by stimulated Raman-type process with two lasers.

IV. CONCLUSION

In conclusion, we have shown that alkaline-earth-metal ions immersed in Bose-Einstein condensates of alkali-metal atoms can give rise to a variety of cold chemical reactions. We have analyzed in detail the elastic and inelastic processes that can occur in a system of a beryllium ion interacting with cold lithium atoms. We have predicted the formation of translationally and rotationally cold $(LiBe)^+$ molecular ions by PA. Theoretical understanding of low-energy atom-ion scattering and reactions may be important for probing dynamics of quantum gases. Since both Bose-Einstein condensation and fermionc superfluidity have been realized in atomic gases of lithium, understanding cold collisions between lithium and beryllium ion may be helpful in probing both bosonic and fermionic superfluidity. In particular, this may serve as an important precursor for generating and probing a vortex ring in lithium quantum gases.

ACKNOWLEDGMENTS

A.R. is grateful to CSIR, Government of India, for a support. We are thankful to P. Ghosh, Presidency College, Kolkata, for his help in computation.

[1] R. P. Stutz and E. A. Cornell, Bull. Am. Soc. Phys. **89**, 76 (2004).
[2] E. R. Meyer, J. L. Bohn, and M. P. Deskevich, Phys. Rev. A **73**, 062108 (2006); E. R. Meyer and J. L. Bohn, *ibid.* **78**, 010502(R) (2008); **80**, 042508 (2009).
[3] J. C. J. Koelemeij, B. Roth, A. Wicht, I. Ernsting, and S. Schiller, Phys. Rev. Lett. **98**, 173002 (2007).
[4] S. Schiller and V. Korobov, Phys. Rev. A **71**, 032505 (2005).
[5] I. W. M. Smith, *Low Temperature and Cold Molecules* (Imperial College Press, London, 2008).
[6] T. Schneider, B. Roth, H. Duncker, I. Ernsting, and S. Schiller, Nat. Phys. **6**, 275 (2010).
[7] E. R. Hudson, Phys. Rev. A **79**, 032716 (2009).
[8] P. F. Staanum, K. Hojbjerre, P. S. Skyt, A. K. Hansen, and M. Drewsen, Nat. Phys. **6**, 271 (2010).
[9] B. Roth, P. Blythe, H. Daerr, L. Patacchini, and S. Schiller, J. Phys. B **39**, S1241 (2006); B. Roth, A. Ostendorf, H. Wenz and S. Schiller, *ibid.* **38**, 3673 (2005).
[10] A. Ostendorf, C. B. Zhang, M. A. Wilson, D. Offenberg, B. Roth, and S. Schiller, Phys. Rev. Lett. **97**, 243005 (2006).
[11] K. Mølhave and M. Drewsen, Phys. Rev. A **62**, 011401 (2000).
[12] V. S. Bagnato, J. Weiner, P. S. Julienne, and C. J. Williams, Laser Phys. **4**, 1062 (1994).
[13] P. L. Gould, P. D. Lett, P. S. Julienne, W. D. Phillips, H. R. Thorsheim, and J. Weiner, Phys. Rev. Lett. **60**, 788 (1988).
[14] M. E. Wagshul, K. Helmerson, P. D. Lett, S. L. Rolston, W. D. Phillips, R. Heather, and P. S. Julienne, Phys. Rev. Lett. **70**, 2074 (1993).
[15] V. Bagnato, L. Marcassa, C. Tsao, Y. Wang, and J. Weiner, Phys. Rev. Lett. **70**, 3225 (1993).
[16] J. P. Shaffer, W. Chalupczak, and N. P. Bigelow, Phys. Rev. Lett. **82**, 1124 (1999).
[17] J. C. Pearson, L. C. Oesterling, E. Herbst, and F. C. De Lucia, Phys. Rev. Lett. **75**, 2940 (1995).
[18] I. S. Vogelius, L. B. Madsen, and M. Drewsen, Phys. Rev. A **70**, 053412 (2004); J. Phys. B **39**, S1267 (2006); K. Højbjerre, A. K. Hansen, P. S. Skyt, P. F. Staanum, and M. Drewsen, New J. Phys. **11**, 055026 (2009).
[19] W. W. Smith, O. P. Marakov, and J. Lin, J. Mod. Opts. **52**, 2253 (2005).
[20] C. Zipkes, S. Palzer, C. Sias, and M. Kohl, Nat. Lett. **464**, 388 (2010).
[21] C. Zipkes, S. Palzer, L. Ratschbacher, C. Sias, and M. Kohl, Phys. Rev. Lett. **105**, 133201 (2010).
[22] A. T. Grier, M. Cetina, F. Oručević, and V. Vuletić, Phys. Rev. Lett. **102**, 223201 (2009).
[23] J. Weiner, V. S. Bagnato, S. Zilio, and P. S. Julienne, Rev. Mod. Phys. **71**, 1 (1999); K. M. Jones, E. Tiesinga, P. D. Lett, and P. S. Julienne, *ibid.* **78**, 483 (2006).
[24] S. Schmid, A. Harter, and J. H. Denschlag, Phys. Rev. Lett. **105**, 133202 (2010).
[25] E. Bodo, P. Zhang, and A. Dalgarno, New J. Phys. **10**, 033024 (2008).
[26] P. Zhang, E. Bodo, and A. Dalgarno, J. Phys. Chem. A **113**, 15085 (2009).
[27] Peng Zhang, Alex Dalgarno, and Robin Côté, Phys. Rev. A **80**, 030703(R) (2009).
[28] Z. Idziaszek, T. Calarco, P. S. Julienne, and A. Simoni, Phys. Rev. A **79**, 010702(R) (2009).
[29] B. Gao, Phys. Rev. Lett. **104**, 213201 (2010).
[30] R. Côté and A. Dalgarno, Phys. Rev. A **62**, 012709 (2000).
[31] O. P. Makarov, R. Côté, H. Michels, and W. W. Smith, Phys. Rev. A **67**, 042705 (2003).
[32] X. Ma *et al.*, J. Phys.: Conf. Ser. **88**, 012019 (2007).
[33] R. Côté, Phys. Rev. Lett. **85**, 5316 (2000).
[34] P. Massignan, C. J. Pethick, and H. Smith, Phys. Rev. A **71**, 023606 (2005).
[35] R. M. Kalas and D. Blume, Phys. Rev. A **73**, 043608 (2006).
[36] F. M. Cucchietti and E. Timmermans, Phys. Rev. Lett. **96**, 210401 (2006).
[37] R. Côté, V. Kharchenko, and M. D. Lukin, Phys. Rev. Lett. **89**, 093001 (2002).
[38] A. A. Safonov, V. F. Khrustov, and N. F. Stepanov, Zhurnal Strukturnoi Khimii **24**, 168 (1983).
[39] D. D. Konowalow and M. E. Rosenkrantz, Chem. Phys. Lett. **61**, 489 (1979).
[40] D. L. Cooper, K. Kirby, and A. Dalgarno, Canadian J. Phys. **62**, 1622 (1984).
[41] B. Zygelman and A. Dalgarno, Phys. Rev. A **38**, 1877 (1988).
[42] B. Zygelman, A. Dalgarno, M. Kimura, and N. F. Lane, Phys. Rev. A **40**, 2340 (1989).
[43] P. C. Stancil and B. Zygelman, Astro. J. **472**, 102 (1996).
[44] B. W. West, N. F. Lane, and J. S. Cohen, Phys. Rev. A **26**, 3164 (1982).
[45] H. R. Thorsheim, J. Weiner, and P. S. Julienne, Phys. Rev. Lett. **58**, 2420 (1987); A. Hansson and J. K. G. Watson, J. Mol. Spec. **233**, 169 (2005).
[46] B. R. Johnson, J. Chem. Phys. **67**, 4086 (1977).